

Article

Chloroform Fraction of *Prasiola japonica* Ethanolic Extract Alleviates UPM 1648a-Induced Lung Injury by Suppressing NF- κ B Signaling

Sang Hee Park ^{1,†} , Ji Hye Kim ^{2,3,†} , Minkyung Song ², Hwa Pyoung Lee ², Ji Hye Yoon ¹, Dong Seon Kim ², Seok Gu Jang ⁴, Dong Sam Kim ^{4,*} and Jae Youl Cho ^{1,2,3,*} 

¹ Department of Biocosmetics, Sungkyunkwan University, Suwon 16419, Republic of Korea

² Department of Integrative Biotechnology, Sungkyunkwan University, Suwon 16419, Republic of Korea

³ Biomedical Institute for Convergence at SKKU (BICS), Sungkyunkwan University, Suwon 16419, Republic of Korea

⁴ Samcheok *Prasiola japonica* Research Center, Samcheok City Hall, Samcheok 25914, Republic of Korea

* Correspondence: prasiolra@korea.kr (D.S.K.); jaecho@skku.edu (J.Y.C.); Tel.: +82-31-290-7876 (J.Y.C.)

† These authors contributed equally to this work.

Abstract: *Prasiola japonica* is an edible alga, and the ethanol extract of *P. japonica* (Pj-EE) possesses various biological activities. Interestingly, in a recent study, we observed the potent anti-inflammatory activity of the chloroform fraction of Pj-EE (Pj-EE-CF). Thus, to extend the application of Pj-EE-CF, we further studied its effects on lung injury. To establish an experimental model of lung injury, we nasally administered urban particulate matter UPM 1648a (50 mg/kg) to mice. In addition, BEAS-2B cells were treated with 300 μ g/mL of UPM 1648a for in vitro analysis. Intranasal administration of UPM 1648a increased lung injury score, macrophage infiltration, and upregulation of the inflammatory enzyme inducible nitric oxide synthase (iNOS) in lung tissues. On the other hand, oral administration of Pj-EE-CF (25, 50, and 100 mg/kg) alleviated these pathological features as assessed by lung wet/dry ratio, lung injury score, bronchoalveolar lavage fluid (BALF) protein amount in the lung tissues up to 70%, 95%, and 99%, respectively. In addition, Pj-EE-CF down-regulated the release of inflammatory cytokines, interleukins (ILs), tumor necrosis factor (TNF)- α , and interferon (IFN)- γ elevated by UPM 1648a in the lung tissues and lung BALF up to 95%. According to Western blot and luciferase assay, Pj-EE-CF (100 mg/kg in vivo or 50 and 100 μ g/mL in vitro) significantly reduced the nuclear factor- κ B (NF- κ B) signal activated by UPM 1648a. Finally, UPM 1648a increased cellular reactive oxygen species (ROS) levels in BEAS-2B cells, while Pj-EE-CF reduced them. These results suggest that Pj-EE-CF alleviates UPM 1648a-induced lung damage via anti-inflammatory and antioxidant activities and by suppressing NF- κ B signaling. In conclusion, these observations imply that Pj-EE-CF could be a practical component of food supplements to mitigate air pollution-derived lung damage.

Keywords: urban particulate matter; air pollution; lung damage; *Prasiola japonica*; anti-inflammatory; NF- κ B



Citation: Park, S.H.; Kim, J.H.; Song, M.; Lee, H.P.; Yoon, J.H.; Kim, D.S.; Jang, S.G.; Kim, D.S.; Cho, J.Y. Chloroform Fraction of *Prasiola japonica* Ethanolic Extract Alleviates UPM 1648a-Induced Lung Injury by Suppressing NF- κ B Signaling. *Foods* **2023**, *12*, 88. <https://doi.org/10.3390/foods12010088>

Academic Editor: Kuiwu Wang

Received: 13 October 2022

Revised: 15 December 2022

Accepted: 21 December 2022

Published: 24 December 2022



Copyright: © 2022 by the authors. Licensee MDPI, Basel, Switzerland. This article is an open access article distributed under the terms and conditions of the Creative Commons Attribution (CC BY) license (<https://creativecommons.org/licenses/by/4.0/>).

1. Introduction

Algae, aquatic photosynthetic organisms, contain abundant bioactive compounds such as polyphenols, phycobiliproteins, and vitamins with numerous medicinal effects, including antioxidant, anticancer, and antiviral properties and are of interest in the pharmaceutical industry [1]. Algae (especially chlorophyte and Bryophyta algae) are a valuable source of dietary supplements such as omega-3 polyunsaturated fatty acids (PUFA), β -carotene, astaxanthin, and carotenoids [1]. *Prasiola* is a genus of leafy green algae that inhabit freshwater, terrestrial, and marine environments. A total of 36 species of the genus *Prasiola* have been reported, of which 14 are freshwater species [2]. In Korea, Park et al. found a *Prasiola* species in Samcheok, Gangwon-do, in 1970 [3], and this was later identified

as *P. japonica*, distributed in Korea and Japan as traditionally edible algae [4]. Pharmaceutical benefits such as antioxidant, anti-inflammatory, and skin-protective effects have been confirmed in various in vitro and in vivo models [5–7].

In a recent study, we compared the general anti-inflammatory effects of solvent fractions of Pj-EE prepared with n-hexane, chloroform, n-butanol, and water [8]. Interestingly, the chloroform fraction (Pj-EE-CF) was most effective in suppressing nitric oxide levels and inflammatory cytokine gene expression in LPS-stimulated macrophages and in reducing edema in carrageenan-treated paws [8]. The predominantly used indicators in the evaluation of the inflammatory activities of compounds or plant-derived extracts are influenced by Pj-EE [9–11]. Thus, we further studied the application of Pj-EE-CF in other inflammation-related diseases in this study. Among many diseases, we examined a model of lung disease, which has become a serious problem in Korea due to the explosive accumulation of air pollution, including particulate matter [12,13].

Air pollution is a major health threat worldwide. Numerous published works indicate that exposure to air pollution is associated with increased respiratory and vascular disease and leads to high morbidity and mortality [14,15]. The components of air pollution vary depending on the source but mainly include particulate matter (PM), nitrogen dioxide (NO₂), sulfur dioxide (SO₂), and ozone (O₃) [16]. Recently, the danger of PM has been emphasized [17]. PM is a mixture of inorganic and organic particles and is classified according to particle size as ultrafine (diameter ≤ 0.1 μm, PM0.1), fine (diameter ≤ 2.5 μm, PM2.5), and coarse particles (diameter ≤ 10 μm, PM10). [18]. PM10 is efficiently deposited in the upper respiratory tract by impaction or gravitational sedimentation [19]. PM2.5, also known as fine dust, can penetrate the alveolar area by diffusion and deposition, affecting the respiratory, cardiovascular, and nervous systems [20]. Furthermore, PM2.5 inhaled into the respiratory tract affects lung macrophages and epithelia [21–24]. In addition, PM2.5 induces excessive oxidative stresses and reactive oxygen species (ROS)-dependent systemic inflammation [25,26]. Moreover, epidemiological works have shown that PM2.5 increases the risk of *Pseudomonas aeruginosa* (*P. aeruginosa*) infection and pneumonia [21,22,24]. Despite these harmful effects, studies on molecular mechanisms and methods to prevent and reduce PM-derived health problems are limited. Urban particulate matter (UPM) 1648a is a commonly used material for in vivo and in vitro experimental studies regarding exposure to air pollution. According to the literature [27,28], UPM 1648a impairs the cardiovascular system and skin barrier function and causes oxidative stress. In addition, UPM 1648a has been reported to exacerbate arthritis and induce hyperinflammatory responses [29,30]. In our study, nasal administration of UPM 1648a also increased the levels of cytokines in the lung tissues and BALF, leading to lung injury. This evidence indicates that the UPM 1648a-induced lung injury model is suitable for testing the anti-inflammatory effect of Pj-EE-CF. Therefore, we evaluated the health benefits of Pj-EE-CF using this model and also evaluated the anti-inflammatory mechanism of Pj-EE-CF against lung inflammation caused by UPM1648a using the BEAS-2B cell line (a human bronchial epithelial cell line).

2. Materials and Methods

2.1. Materials

BEAS-2B cells (ATCC number CRL-9609) were purchased from American Type Culture Collection (ATCC) (Rockville, MD, USA). UPM 1648a (NIST SRM 1648a) was obtained from the National Institute of Standards and Technology (NIST, USA). According to the certificate of analysis provided by the NIST, UPM 1648a was collected in the St. Louis, MO area over a certain period (1976–1977). Collected materials were combined into a single lot, and extraneous materials were removed through a fine-meshed sieve and then blended with a V-blender. The composition and homogeneity of UPM 1648a are continuously monitored by the NIST for quality assurance. Dimethyl sulfoxide (DMSO), sodium dodecyl sulfate (SDS), and 3-(4,5-dimethylthiazol-2-yl)-2,5-diphenyltetrazolium bromide (MTT) were purchased from Sigma-Aldrich Co. DMEM, penicillin–streptomycin, trypsin, and phosphate-buffered saline, were purchased from HyClone (Logan, UT, USA). Fetal bovine serum (FBS) was

obtained from Biotechnics Research, Inc. (Irvine, CA, USA). TRIzol reagent was purchased from MRCgene (Cincinnati, OH, USA). The enzyme-linked immunosorbent assay (ELISA) kits for IL-1 β (MLB00C), IL-6 (M6000B), TNF- α (MTA00B), IL-4 (M4000B), IL-12 (M1270), and IFN- γ (MIF00) were obtained from R&D Systems (Minneapolis, MN, USA). Cell lysis buffer and phospho-specific or total-protein antibodies against I κ B α , p-50, p65, and β -actin were obtained from Cell Signaling Technology (Beverly, MA, USA).

2.2. Pj-EE and Fraction Preparation

P. japonica was provided by the *Prasiola japonica* Research Center (Samcheok City, Gangwon-do, Republic of Korea). First, the dried sample was cut into 1 mm samples, and 70% ethanol was added at a ratio of 1:20 (*w/v*) to extract for 24 h. Then, the supernatant, excluding the precipitate, was filtered using a 110 nm filter paper (No. 2, Advantec, Toyo Co., Tokyo, Japan), and ethanol remaining in the solution was removed through a vacuum concentrator (Eyela New Rotary Vacuum Evaporator, Rikakikai Co., Tokyo, Japan). Finally, the sample was dried by a vacuum freeze dryer (Eyela FD1, Rikakikai Co., Tokyo, Japan) for 72 h [31,32]. The total sample weight was 310 g, the extracted amount was 33.143 g, and the yield was 10.69%. As shown in Figure 1A, the ethanol extract of *P. japonica* was fractionated using n-hexane, chloroform, n-butanol, and water. The yields of these preparations were 1.27% (hexane fraction), 0.63% (chloroform fraction), 0.67% (butanol fraction), and 7.47% (water fraction). The dried samples were stored in a $-20\text{ }^{\circ}\text{C}$ freezer.

2.3. Cell Culture and Cell Viability Assay

Human bronchial epithelial BEAS-2B cells were cultured in DMEM containing 10% FBS, 100 mg/mL streptomycin, and 100 U/mL penicillin at $37\text{ }^{\circ}\text{C}$ in a 5% CO_2 humidified incubator. BEAS-2B cells (5×10^4 cells/mL) were seeded in a 96-well plate and treated with Pj-EE-CF (0–100 $\mu\text{g/mL}$) for 24 h. To test the cytoprotective activity of Pj-EE-CF (0–100 $\mu\text{g/mL}$), we treated BEAS-2B cells with Pj-EE-CF and UPM 1648a (300 $\mu\text{g/mL}$) or UPM 1648a (300 $\mu\text{g/mL}$) alone for 24 h. A conventional MTT assay determined cell viability and cytoprotective activity [33,34].

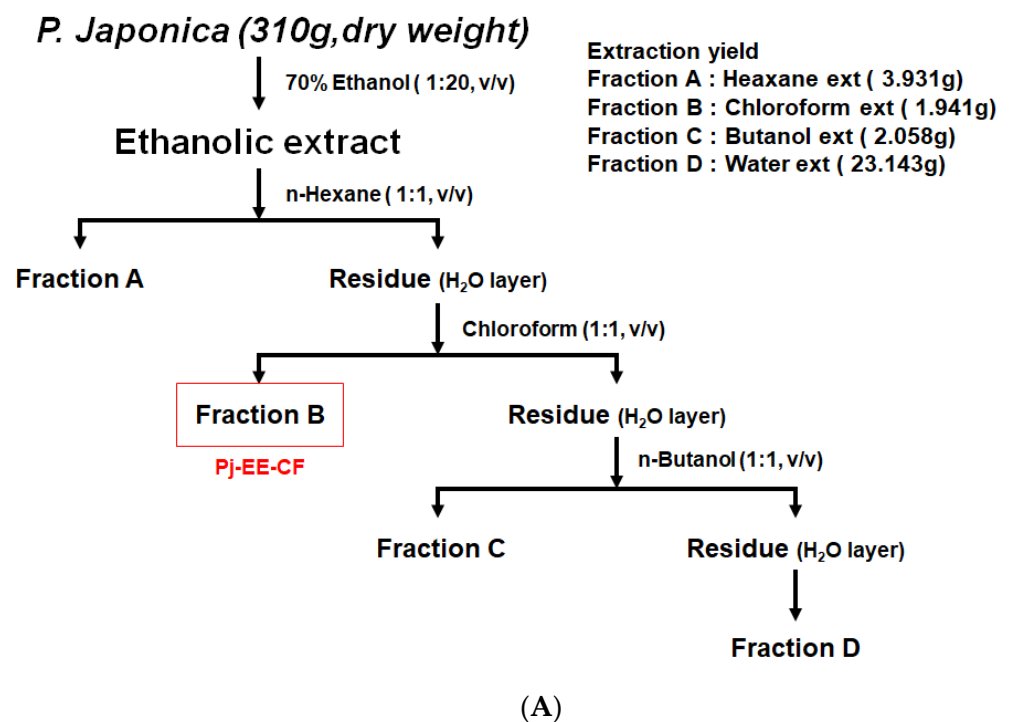


Figure 1. Cont.

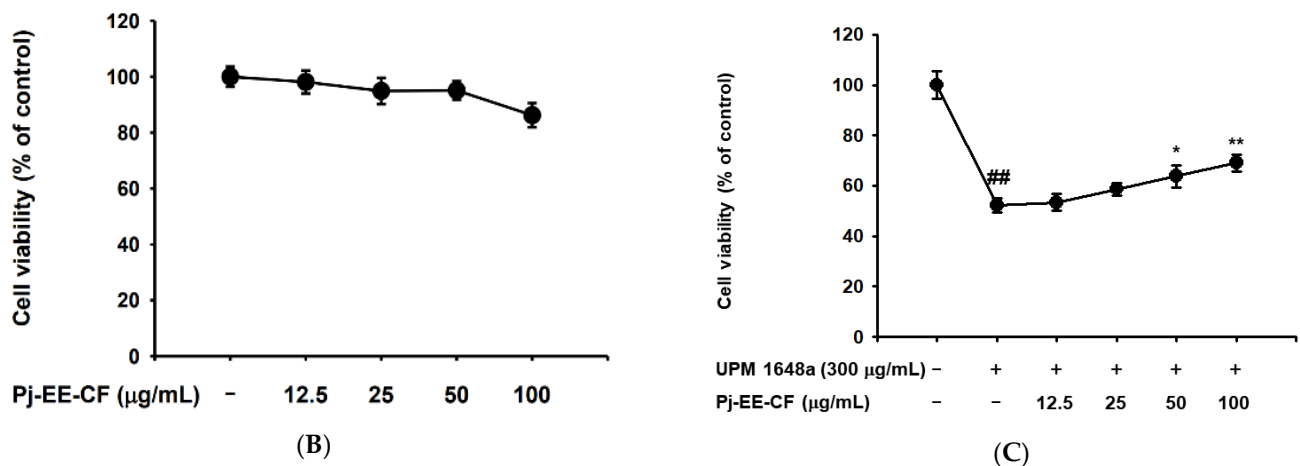


Figure 1. Cytotoxicity and cytoprotective effects of Pj-EE-CF in BEAS-2B human bronchial epithelial cells. (A) Fractionation diagram of the various solvents of *P. japonica* ethanolic extract (Pj-EE). (B,C) BEAS-2B cells were treated with UPM1648a (300 µg/mL) and Pj-EE-CF (0–100 µg/mL) or Pj-EE-CF (0–100 µg/mL) alone for 24 h. Cell viability was analyzed analytically by MTT. Data in (B,C) are presented as mean \pm SD of six replicates ($n = 6$). ## $p < 0.01$ compared to normal (non-treatment), * $p < 0.05$ and ** $p < 0.01$ compared to control (UPM 1648a alone).

2.4. Animals

ICR mice (8 weeks old, male, 20–21 g) were purchased from Orient Bio (Sunngam, Korea) and bred at SKKU animal holding facility. Breeding facilities are pathogen-free, maintain a constant temperature (21–23 °C) and constant humidity (45–60%), and maintain a 12 h light/dark cycle. The mice were divided into five study groups, the control (vehicle) group, UPM1648a (50 mg/50 µL) group, and three groups representing UPM 1648a exposure (50 mg/50 µL) + Pj-EE-CF (25, 50, and 100 mg/kg), with five mice per group. The control mice were orally administered saline. UPM mice were intranasal administration with 50 µL of PBS containing 50 mg/mL UPM1648a for 3 days. For accurate intranasal administration, all mice were anesthetized just before intranasal administration. Mice in the UPM + Pj-EE-CF groups were given Pj-EE-CF (25–100 mg/kg) orally twice per day for three days, once an hour before UPM1648a treatment and once an hour after UPM1648a treatment. Mice were sacrificed after three days. BALF and lung samples were isolated. BALF was immediately collected, and all lobes of each lung were harvested. The collected BALF was used for ELISA analysis, and the largest left lobe of the lung was used for wet/dry ratio analysis. The middle and lower lobes were used for histopathological data, and the upper lobes were used for Western blotting. All animal experiments were performed in accordance with the guidelines established by the Institutional Animal Care and Use Committee (IACUC) of Sungkyunkwan University (IACUC No.: SKKUIACUC2021-04-12-1).

2.5. Lung Wet-to-Dry Weight Ratio and Protein Concentration Ratio Measurement

The left lobes of mouse lung tissue were washed with PBS. After recording the wet weight, the lung tissue was dried using an oven at 60 °C for 72 h, and the weight of the dried lung tissue was measured. Wet-to-dry ratios were calculated to assess the degree of inflammation in the lung tissue [35,36]. The protein concentration ratio was analyzed using the collected BALF. The protein concentration of the collected BALF was analyzed using the Bradford protein quantification method, and the analyzed result was quantified using a protein concentration standard curve. A protein concentration standard curve was determined by dissolving BSA (0–4 mg/mL) in PBS.

2.6. Histological Analysis of Lung Tissue

The right lobes of the mouse lung were harvested and fixed in 4% formalin solution for 2 days. The fixed samples were embedded with paraffin, cut to a thickness of 3 µm,

and then stained with Hematoxylin & Eosin. Lung injury was assessed by analyzing septal thickening of the alveolar walls, neutrophil infiltration, and membrane structure formation composed of cell debris according to a previously published paper [36,37] and as described in Table 1.

Table 1. Lung injury scoring index [37].

Measurement Criteria	Score		
	0	1	2
A. Neutrophil infiltration into the interstitial space	Not found	1 to 5	More than 5
B. Neutrophil infiltration into the alveolar space	Not found	1 to 5	More than 5
C. Number of hyaline membranes	Not found	3	More than 3
D. Septal thickening of the alveolar wall	More than 2×	2 to 4×	More than 4×
Score = [(20 × A) + (14 × B) + (7 × C) + (2 × D)] / (field number × 100)			

2.7. ELISA in BALF and Lung Tissue Lysate

Then, 500 µL BALF was extracted from the trachea of each mouse with 100 µM EDTA in 1 mL PBS. It was prepared at the same concentration for each group ($n = 5$ /group) by adjusting with PBS based on Bradford assay. To obtain the lung tissue lysates, lung tissue was lysed by treating cell lysis buffer and homogenized with sonicator [36]. Tissue lysates were centrifuged at $11,000 \times g$ for 5 min at 4 °C, and supernatants were used for ELISA. Protein concentrations of IL-1 β , IL-4, IL-6, IL-12, IFN- γ , and TNF- α in BALF and lung tissues were determined according to the manufacturer's instructions.

2.8. Whole-Cell Lysate Preparation and Western Blotting Analysis

Lung tissue was lysed with cell lysis buffer and sonicated for whole cell lysates. Cell lysates obtained by homogenization were centrifuged at $11,000 \times g$ for 5 min at 4 °C, and supernatants were used for Western blotting analysis. Protein samples were separated by protein size through SDS-polyacrylamide gel electrophoresis. The gel containing the proteins was transferred to a polyvinylidene fluoride (PVDF) membrane. The first antibody was attached to total and phosphorylated proteins. A secondary antibody recognizing the first antibody was added. It was visualized using an enhanced chemiluminescence reagent.

2.9. Luciferase Reporter Gene Activity

Regarding the luciferase reporter assays, baes-2b cells (2×10^5 cells/mL in 12-well plates) were transfected with 1 µg of plasmid-containing β -galactosidase and NF- κ B-1-Luciferase reporter gene using lipofectamine 2000 (Thermo Fisher Scientific, Waltham, MA, USA). The cells were incubated with Pj-EE-CF (0–100 µg/mL) and UPM 1648a (300 mg/mL) or UPM 1648a (300 µg/mL) alone for 24 h. The cells were lysed using a cell lysis buffer reacted with luciferin to generate fluorescence, and then fluorescence was measured using a luminescence spectrophotometer. Normalization of the luciferase reporter assay was performed through the activity of β -galactosidase [38].

2.10. Cellular ROS Assay

BEAS-2B cells were dispensed in a 12-well plate to be 1.5×10^5 cells/well and cultured using a 5% CO₂ incubator for 24 h. Cells were treated with Pj-EE-CF (0–50 µg/mL) and UPM 1648a (300 µg/mL) or UPM 1648a (300 µg/mL) alone. After 24 h, the cultured cells were washed three times with PBS and stained with H2DCF-DA (10 µM). The stained cells were analyzed using a CytoFLEX Flow Cytometer, and fluorescence was analyzed (Beckman Coulter Life Sciences, Indianapolis, IN, USA) [32,39].

2.11. Statistical Analysis

All the results of our study were calculated as mean ± standard deviation (SD) of an experiment performed with six (Figures 1B,C, and 5E), five (Figures 2B,D–G, 3, and 4) or three (Figure 5B–D) replicates per group. Our results were analyzed by ANOVA, Scheffe’s post-hoc test, and Mann–Whitney U test to analyze statistical significance. Results with values less than 0.05 in the analyzed *p*-values were considered statistically significant in all analyses. (# *p* < 0.05, ## *p* < 0.01, * *p* < 0.05, ** *p* < 0.01). All statistical analyses were conducted using the Statistical Package for the Social Sciences program (IBM Corp., Armonk, NY, USA).

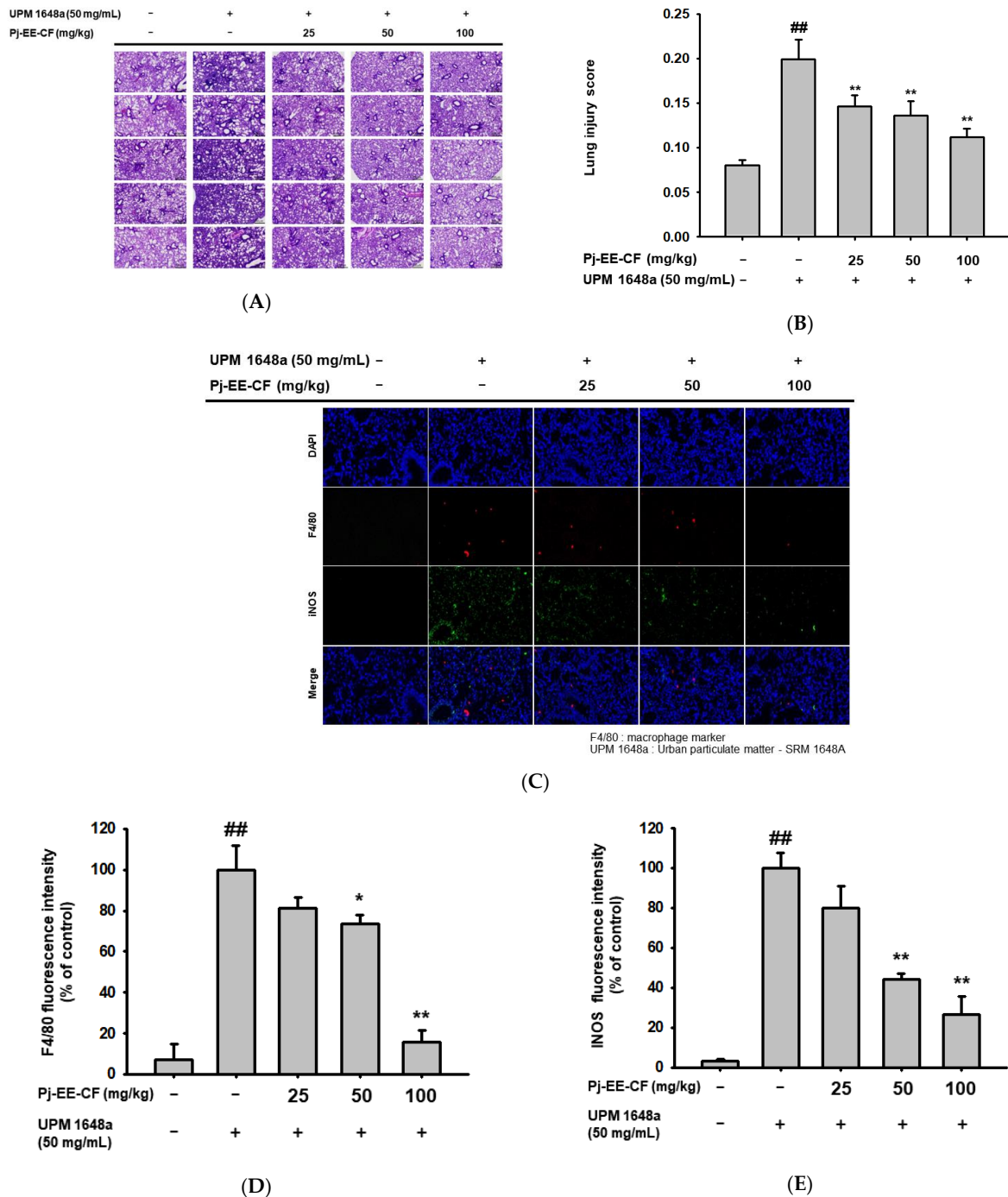


Figure 2. Cont.

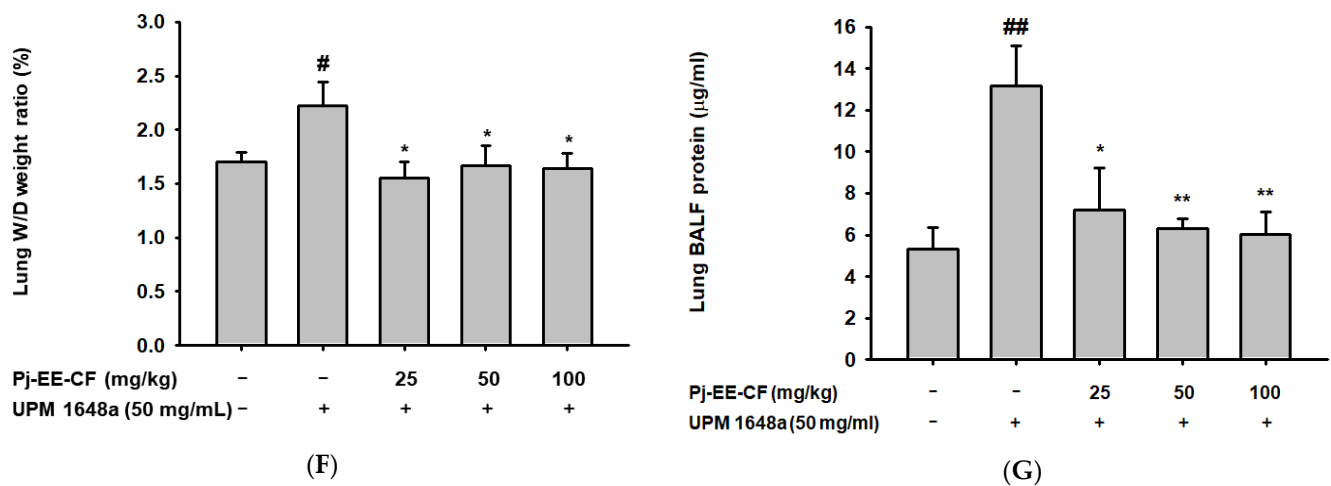


Figure 2. Pulmonary pathological alteration after UPM 1648a instillation and Pj-EE-CF administration in mice. (A) Representative image of the pathologic features of lung tissues prepared with five mice per group. Lung tissues from UPM 1648a and Pj-EE-CF treated mice were H&E stained. (B) Lung injury score of pulmonary tissue in each group. (C) A fluorescence microscopy image of macrophage and iNOS in lung tissue. Immunofluorescence was employed to assess macrophage infiltration (F4/80: red) and iNOS (green), and nuclei were stained with DAPI (blue). (D,E) Quantification of fluorescence intensity. Fluorescence intensities of F4/80 and iNOS were analyzed using Image J software and fluorescence intensities relative to control were calculated as percentage and expressed as mean \pm SD. (F) Lung wet/dry (W/D) ratio in each group. The pulmonary water content was investigated by analyzing the lung W/D ratio. (G) Protein concentration in BALF prepared from UPM 1648a-exposed mice orally pretreated with Pj-EE-CF (25–100 mg/kg) was determined by the Bradford assay. All assays depicted in (A–G) were performed with five mice per group. Results (B,D–G) are presented as mean \pm SD. # $p < 0.05$ and ## $p < 0.01$ compared to normal (non-treatment), * $p < 0.05$ and ** $p < 0.01$ compared to control (UPM 1648a alone).

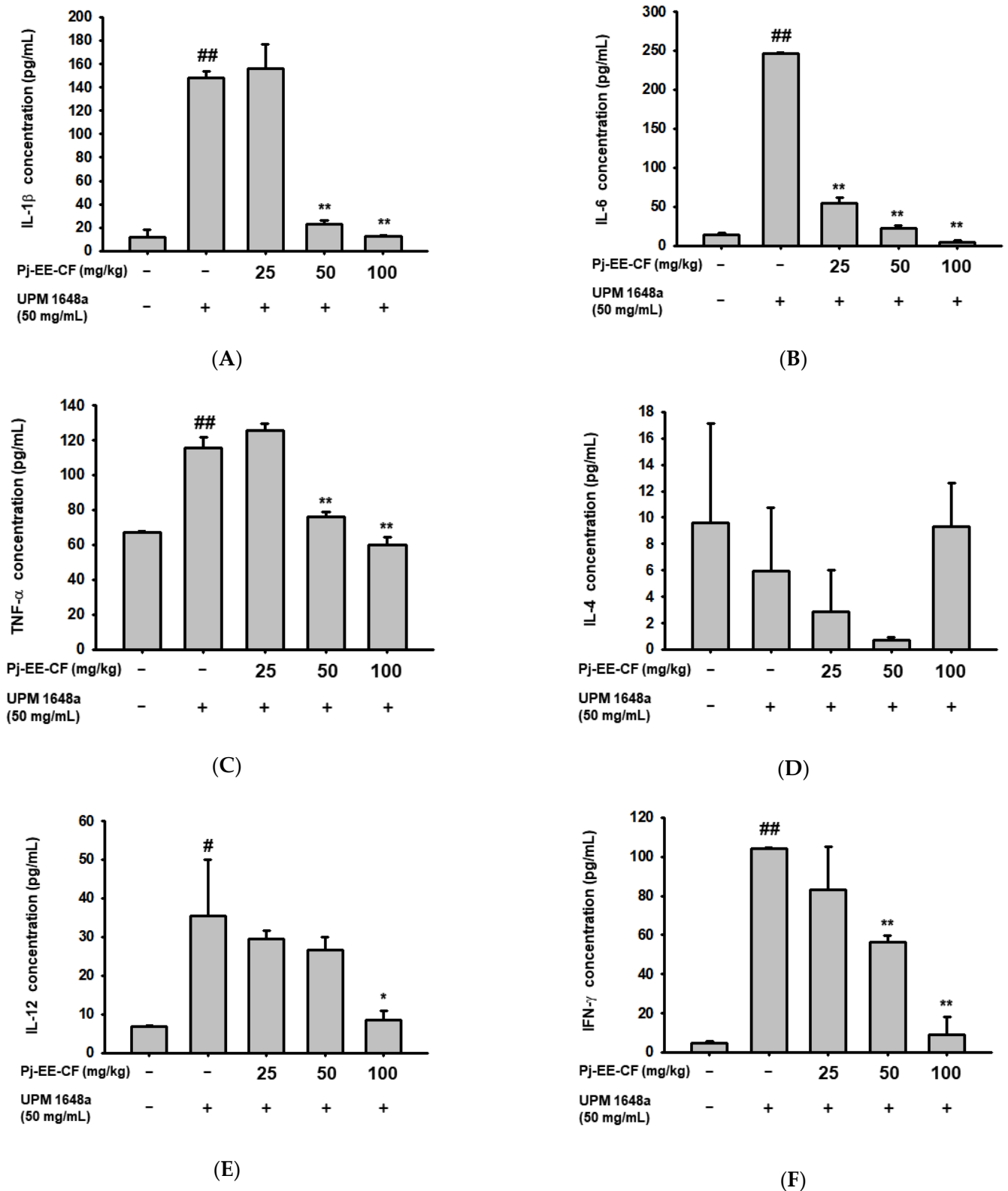


Figure 3. Inflammatory cytokine levels in BALF after UPM 1648a instillation and Pj-EE-CF administration in mice. IL-1 β (A), IL-6 (B), TNF- α (C), IL-4 (D), IL-12 (E), and IFN- γ (F) concentrations were determined by ELISA with BALF, using the same amount of protein as adjusted with PBS. All data are presented as mean \pm SD of five biological replicates ($n = 5$ mice/group). # $p < 0.05$ and ## $p < 0.01$ compared to normal (non-treatment), * $p < 0.05$ and ** $p < 0.01$ compared to control (UPM 1648a alone).

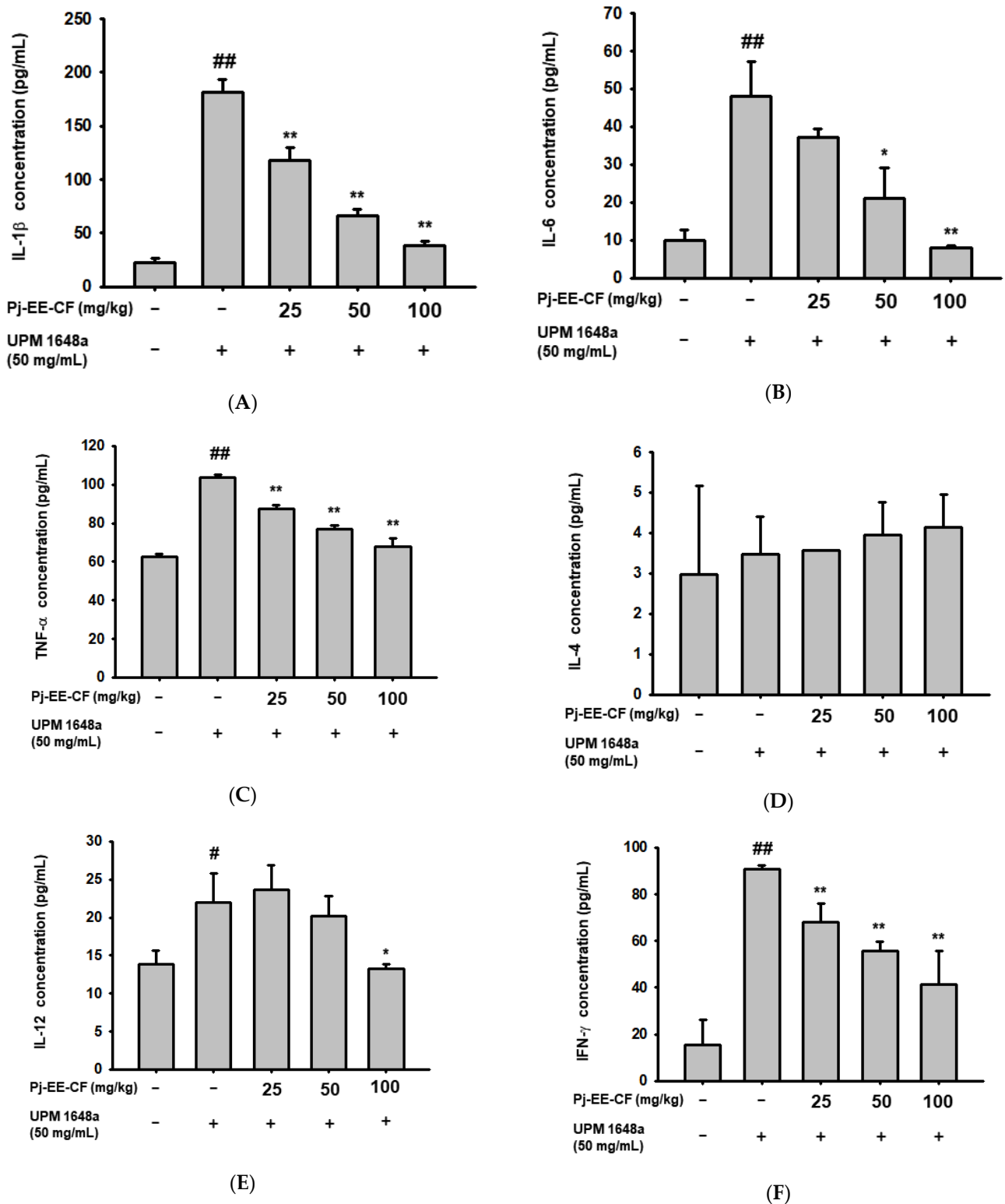


Figure 4. Inflammatory cytokine levels in mouse lung tissue homogenates after UPM 1648a instillation and Pj-EE-CF administration. IL-1 β (A), IL-6 (B), TNF- α (C), IL-4 (D), IL-12 (E), and IFN- γ (F) concentrations were determined by ELISA with lung lysates of 5 mice. All data are presented as mean \pm SD (standard deviation) of the five biological replicates (n = 5 mice/group). # $p < 0.05$ and ## $p < 0.01$ compared to normal (non-treatment), * $p < 0.05$ and ** $p < 0.01$ compared to control (UPM 1648a alone).

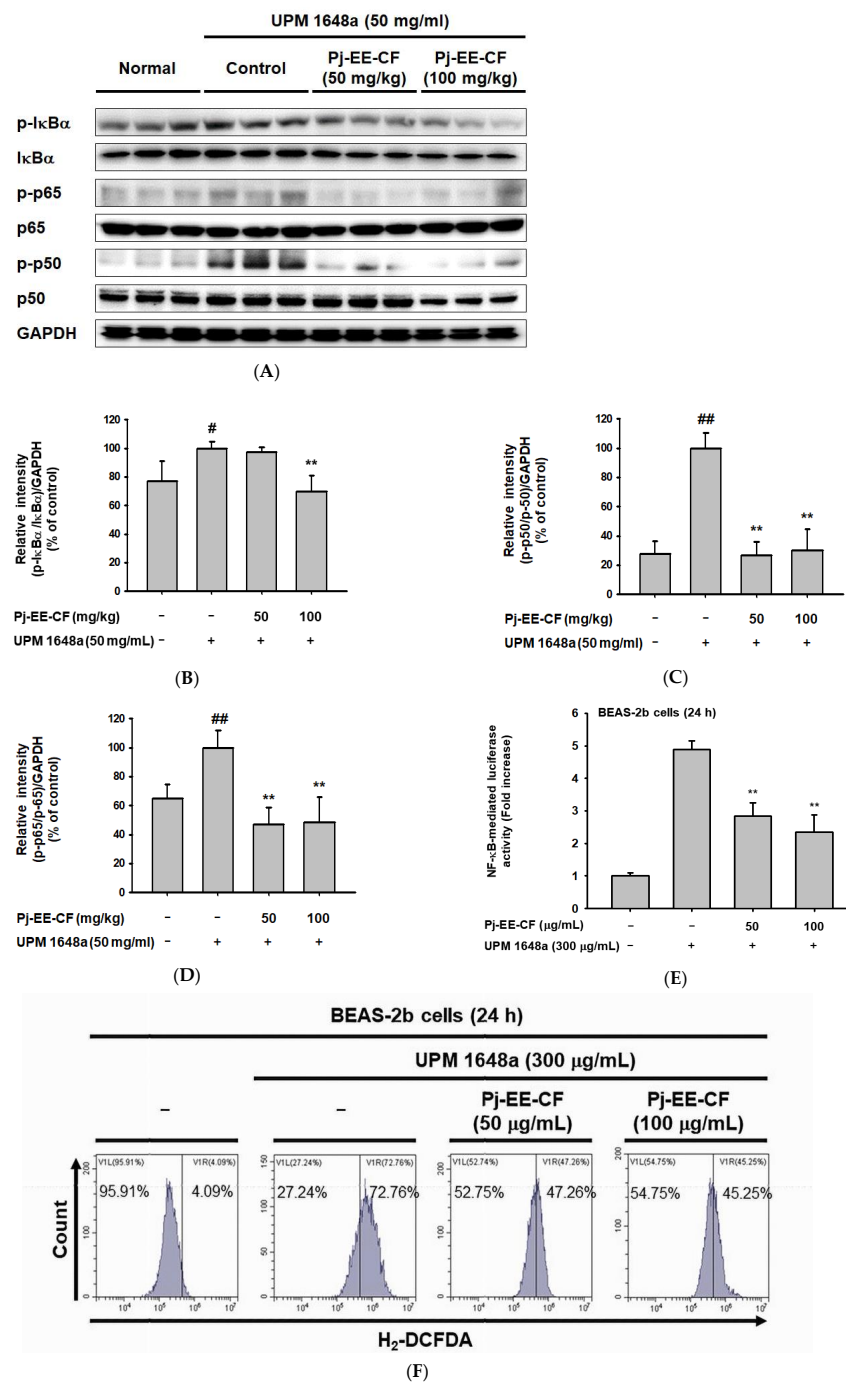


Figure 5. Inhibition of NF-κB signal by Pj-EE-CF. **(A)** Immunoblots of NF-κB signal molecules (IκBα, p65, p50) in UPM 1648a- and Pj-EE-CF-treated mouse lung tissues. Immunoblot images show all three biological replicates. NF-κB pathway-related molecules were detected using antibodies for total and phospho-forms of IκBα, p50, and p65. **(B–D)** Band intensity of the immunoblots was measured and quantitated through Image J software, and the relative intensity of the band is expressed as mean ± SD of the three biological replicates (n = 3 mice/group). **(E)** NF-κB luciferase assay in BEAS-2B cells treated with UPM 1648a (300 μg/mL) and Pj-EE-CF (0–100 μg/mL) or UPM 1648a (300 μg/mL) alone. Data in **(E)** are presented as mean ± SD of the three samples. **(F)** BEAS-2B cells were treated with UPM 1648a (300 μg/mL) and Pj-EE-CF (0–100 μg/mL) or UPM 1648a (300 μg/mL) alone and labeled with DCFDA. Fluorescence of DCFDA was detected by flow cytometry. # *p* < 0.05 and ## *p* < 0.01 compared to normal (non-treatment), ** *p* < 0.01 compared to control (UPM 1648a alone).

3. Results

3.1. Pj-EE-CF Protects UPM 1648a-Exposed Human Bronchial Epithelium Cells

To evaluate the cytotoxicity of Pj-EE-CF, we treated BEAS-2B cells with Pj-EE-CF (0–100 µg/mL) and performed the MTT assay. Pj-EE-CF did not affect the cell viability of BEAS-2B cells up to concentrations of 100 µg/mL (Figure 1B). The cytotoxicity of UPM1648a (150 µg/mL) has been verified in nasal epithelial cells [40]. Consistently, BEAS-2B cell viability was decreased by 50% in the UPM 1648a-treated group (Figure 1C). Interestingly, Pj-EE-CF reversed the BEAS-2B cell viability decreased by UPM 1648a exposure, suggesting that Pj-EE-CF can protect bronchial epithelial cells from UPM 1648a-induced cell damage.

3.2. Pj-EE-CF Alleviates Pathological Changes of Lung Tissues in UPM 1648a-Stimulated Mice

To analyze the effect of Pj-EE-CF, we stained lung tissues from UPM 1648a-treated mice with H&E. The control group showed a typical pattern of histology, while the UPM 1648a group exhibited histological changes. However, oral administration of Pj-EE-CF (25, 50, and 100 mg/kg) alleviated the histopathological changes (Figure 2A). In parallel, UPM 1648a increased histological injury scores, and Pj-EE-CF decreased them (Figure 2B). In addition, the signal intensity of F4/80, a macrophage marker in lung tissues, was significantly increased by UPM 1648a but decreased by Pj-EE-CF (50 and 100 mg/kg) in a concentration-dependent manner under fluorescence microscopy (Figure 2C,D). Consistently, Pj-EE-CF suppressed UPM 1648a-induced iNOS, an inflammatory enzyme mainly expressed by macrophages (Figure 2C,E). Changes in pulmonary vascular permeability were evaluated by analyzing the W/D ratio of the lung. UPM 1648a increased the lung W/D ratio, and Pj-EE-CF reduced the lung W/D ratio to the control level (Figure 2F). In patients with lung disease, particularly asthma, BALF contains more blood proteins than in healthy people due to plasma extravasation [41]. Likewise, UPM 1648a increased BALF protein content, but Pj-EE-CF administration suppressed the BALF protein concentration (Figure 2G).

3.3. Pj-EE-CF Suppresses UPM 1648a-Induced Cytokine Levels in BALF

Next, we analyzed the regulation of Pj-EE-CF on inflammatory cytokines in BALF. The key inflammatory cytokines IL-1 β , IL-6, and TNF- α , were significantly increased in BALF by UPM 1648a (Figure 3A–C). Pj-EE-CF (50, 100 mg/kg) reduced UPM 1648a-induced production of IL-1 β and TNF- α to the control levels (Figure 3A,C). Pj-EE-CF suppressed the level of IL-6 at all treated concentrations (Figure 3B). Pj-EE-CF and UPM 1648a did not alter the production of IL-4, which exerts dual properties (immunostimulatory and immunosuppressive effects) in lung injury and fibrosis (Figure 3D). In addition, Pj-EE-CF affected IL-12 and IFN- γ , which are important inflammatory cytokines in bacterial pneumonia. UPM 1648a increased IL-12 and IFN- γ , and Pj-EE-CF (0–100 mg/kg) dose-dependently decreased the concentrations of the elevated cytokines (Figure 3E,F).

3.4. Pj-EE-CF Decreases UPM 1648a-Induced Cytokine Production in Lung Tissues

As in BALF, treatment with UPM 1648a significantly increased inflammatory cytokines (IL-1 β , IL-6, TNF- α , IL-12, and IFN- γ) in lung tissue. (Figure 4A–C,E,F). Consistent with the results in Figure 3D, IL-4 was not changed by UPM 1648a treatment (Figure 4D). Meanwhile, Pj-EE-CF (0–100 mg/kg) significantly suppressed amounts of IL-1 β , IL-6, TNF- α , and IFN- γ in a concentration-dependent manner (Figure 4A–C,F) but did not affect IL-14 level (Figure 4D). In IL-12, only 100 mg/kg of Pj-EE-CF decreased UPM 1648a-induced IL-12 (Figure 4E).

3.5. Pj-EE-CF Suppresses NF- κ B and Exerts Antioxidant Activity

Since NF- κ B has been reported as the primary transcriptional regulator of pro-inflammatory cytokines [42], we further analyzed the effect of Pj-EE-CF on NF- κ B signal molecules (I κ B α , p65, p50). In resting cells, I κ B α blocks NF- κ B by binding to it and allowing it to remain in the cytoplasm [43]. Upon external stimulation, IKK phosphorylates I κ B α , and the phosphorylated I κ B α is degraded. Sequentially, free NF- κ B subunits p65 and p50 are phos-

phorylated, translocated into the nucleus, and act as transcriptional factors. Interestingly, UPM 1648a significantly increased p-I κ B α level in lung tissues (Figure 5A,B). On the other hand, Pj-EE-CF (100 mg/kg) inhibited the phosphorylation of I κ B α (Figure 5A,B). In addition, the expression levels of p-p50 and p-p65 were upregulated by treatment with UPM 1648a but downregulated by treatment with Pj-EE-CF (50 and 100 mg/kg) (Figure 5A,C,D). We additionally performed a luciferase assay to confirm our hypothesis that Pj-EE-CF affects NF- κ B activity. Consistent with the Western blotting results, UPM 1648a increased NF- κ B-mediated luciferase activity in *BEAS-2B* cells, whereas Pj-EE-CF (50 and 100 μ g/mL) significantly decreased it (Figure 5E). NF- κ B has been reported to increase the expression of pro-oxidant genes such as NADPH oxidase NOX2, iNOS, LOX-12, and LOX-5. [44]. Furthermore, LC-MS performed in our previous work showed that Pj-EE-CF contains abundant flavonoids with antioxidant activities [33]. Thus, we assessed the antioxidant activity of Pj-EE-CF. Cellular ROS levels were detected by flow cytometry in combination with dichlorodihydrofluorescein diacetate (DCFDA), a cell-permeable fluorogenic dye for ROS. As shown in Figure 5F, UPM 1648a increased cellular ROS level, but Pj-EE-CF reduced it, suggesting that decreasing ROS levels may be another possible mechanism involved in the effects of Pj-EE-CF.

4. Discussion

Prolonged inhalation of UPM causes respiratory diseases, including lung injury, but studies on the precise molecular mechanisms for this and on effective drugs or food supplements are lacking [45,46]. UPM, one of the known air pollutants, is emitted into the atmosphere due to fuel combustion and vehicle exhaust and is also formed in natural forms such as volcanic ash and fire [47]. According to the World Health Organization (WHO) Air Quality Guidelines (AQG), continuous exposure to air pollution increases the incidence of chronic respiratory diseases, strokes, and cardiovascular diseases, especially fine dust (PM₁₀, diameter ≤ 2.5 μ m) passes through capillaries to promote inflammatory responses in respiratory system [48]. Furthermore, the WHO's International Agency for Research on Cancer (IARC) has announced that fine dust is the leading cause of lung cancer. Since UPM varies by season and region, in this study, UPM 1648a, administered by intratracheal instillation, was used to achieve repeatability and high stability [49,50]. UPM 1648a contains endotoxin, metal/nonmetal elements, polycyclic aromatic hydrocarbons (PAHs), and polychlorinated biphenyl homologs [51]. The average diameter of UPM 1648a is approximately 5.86 μ m [49], and the size in PBS ranges from 236.43 nm to 1.98 μ m [51].

Uncontrolled inflammation is a pivotal pathophysiologic characteristic of acute lung injury [52,53]. Exposure to external stimuli such as PM and LPS induces the secretion of inflammatory cytokines (IL-1 β , IL-6) in BALF, leading to inflammatory responses [54,55]. TNF- α is a representative cytokine whose expression rapidly increases in acute inflammation and affects pulmonary diseases (asthma, acute lung injury, acute respiratory distress syndrome) [56–58]. IFN- γ elicits Th1-mediated inflammatory responses during acute lung injury, where IL-12 acts as a key upstream regulator of IFN- γ signaling. [59]. Interestingly, UPM 1648a significantly upregulated the cytokines, in particular, IL-1 β , IL-6, and IFN- γ in BALF and lung tissue, while Pj-EE-CF dose-dependently suppressed the increased cytokines. TNF- α and IL-12 also showed an increasing pattern upon UPM 1648a exposure and were decreased by Pj-EE-CF.

NF- κ B plays a pivotal role in a variety of conditions that promote acute lung injury [60]. For example, leukotriene B₄ promotes NF- κ B signaling-induced acute lung injury in a single lung ventilation model [61]. UPM 1648a also induces acute lung injury mediating the NF- κ B [62]. In addition, the intensity and duration of NF- κ B are based on the severity of lung injury in endotoxin-exposed mice [63]. In our previous study, UPM 1648a affected keratinocytes by regulating p38 and NF- κ B pathways [64,65]. Other studies have shown that endotoxin present in UPM increases TLR4-mediated inflammatory responses in murine alveolar macrophages [66,67]. Here, NF- κ B is one of the significant downstream regulators of TLR4 signaling. It has also been reported that several substances exhibit efficacy in

alleviating UPM-induced lung injury through the inhibition of NF- κ B and TLR4 [66,68]. Likewise, Pj-EE-CF suppressed UPM 1648a-induced phosphorylation of NF- κ B signal molecules (I κ B α , p50, p65), alleviating lung inflammation and injury [65,69]. Notably, the inhibitory activity of Pj-EE-CF is so potent that it reduces the p-p50 level increased by UPM 1648a to the basal level. As a result, inhibition of NF- κ B led to the suppression of inflammatory cytokines, such as IL-1, -6, -12, TNF- α , and IFN- γ . On the other hand, Pj-EE-CF did not affect the expression of IL-4 expression regulated by the nuclear factor of activated T cells (NF-AT) or c-maf. Considering these results, Pj-EE-CF seems to selectively inhibit NF- κ B but not NF-AT.

We previously observed that Pj-EE-CF contains approximately 23 active components and flavonoids, including maltol, bavachinin, kushenol N and X, nobiletin, and phel-lochinin [8]. Maltol, bavachinin, and nobiletin have various health benefits, including anti-inflammatory, antioxidant, and anti-tumorigenesis effects, and have shown inhibitory activity of NF- κ B in inflammation models, such as arthritis and endotoxin shock [70–72]. Therefore, the anti-lung injury and NF- κ B inhibitory efficacy of Pj-EE-CF might be derived from the synergistic combination of these flavonoids.

Our results explained the pharmacological efficacy of freshwater laver, edible freshwater green algae. However, it is unclear which components in the chloroform fraction would exhibit pharmacological effects. Therefore, based on the previous studies, we will identify which active compound would inhibit NF- κ B activity by activity-guided fractionation with chloroform fraction using a luciferase assay system. With this information, we will also compare the level of active compound(s) in other fractions as well as crude ethanol extract using mass spectrometry and HPLC analysis. In addition, further research regarding understanding the mechanisms of therapeutic action and molecular target(s) of the fraction will be followed. Finally, although these green algae have been traditionally used, whether the crude extract or fraction of the green algae have side effects in long-term treatment will be carefully examined.

5. Conclusions

In conclusion, Pj-EE-CF mitigated the pathologic features of lung damage, such as lung architecture destruction and lung edema in UPM 1648a-treated mice. In addition, Pj-EE-CF inhibited inflammatory responses via negative regulation of inflammatory cytokine release and macrophage infiltration. Moreover, Pj-EE-CF markedly blocked NF- κ B activation induced by UPM 1648a in lung tissues and BALF. Consequently, our results suggest that the Pj-EE-CF fraction can be a pharmaceutical and food supplement to alleviate UPM 1648a-derived pulmonary damage. Since *P. japonica* is edible algae, the effective consumption amount of raw material was 200 to 900 g to reach its effective dose, according to calculations considering the Pj-EE-CF yield. Therefore, additional studies to improve the extraction yield of active ingredients contained in Pj-EE-CF should be continued to develop functional food preparation with the algae.

Author Contributions: Conceptualization, S.H.P., J.H.K., M.S. and J.Y.C.; data curation, S.H.P. and J.H.K.; formal analysis, S.H.P., J.H.K., M.S., D.S.K. (Dong Sam Kim) and J.Y.C.; funding acquisition, D.S.K. (Dong Sam Kim); investigation, S.H.P., J.H.K., H.P.L., J.H.Y., D.S.K. (Dong Seon Kim), S.G.J. and J.Y.C.; methodology, M.S.; project administration, J.Y.C.; writing—original draft, S.H.P. and J.H.K.; writing—review and editing, M.S., D.S.K. (Dong Sam Kim) and J.Y.C. All authors have read and agreed to the published version of the manuscript.

Funding: This research was supported by Samcheok *Prasiola japonica* Research Center, Samcheok City Hall, Korea (Grant No.: 2021). APC was paid for by the Samcheok *Prasiola japonica* Research Center.

Institutional Review Board Statement: All animal experiments were performed in accordance with the guidelines established by the Institutional Animal Care and Use Committee (IACUC) of Sungkyunkwan University (IACUC No.: SKKUIACUC2021-04-12-1).

Data Availability Statement: The data used to support the findings of this study are available from the corresponding author upon request.

Conflicts of Interest: The authors declare no conflict of interest.

References

1. Aditya, T.; Bitu, G.; Mercy Eleanor, G. The role of algae in pharmaceutical development. *Res. Rev. J. Pharm. Nanotechnol.* **2016**, *4*, 82–89.
2. Moniz, M.B.; Rindi, F.; Guiry, M.D. Phylogeny and taxonomy of prasiolales (trebouxiophyceae, chlorophyta) from Tasmania, including *Rosenvingiella tasmanica* sp. Nov. *Phycologia* **2012**, *51*, 86–97. [[CrossRef](#)]
3. Park, M.; Kim, W.; Chung, I.; Lee, E. Study on the *Prasiola* sp. In Korea. I. Ecological and morphological studies on the *Prasiola* sp. In the Samchuck-Chodang. *Korean J. Bot.* **1970**, *13*, 71–80.
4. Kim, M.S.; Jun, M.-S.; Kim, C.A.; Yoon, J.; Kim, J.H.; Cho, G.Y. Morphology and phylogenetic position of a freshwater Prasiola species (Prasiolales, Chlorophyta) in Korea. *Algae* **2015**, *30*, 197–205. [[CrossRef](#)]
5. Park, S.H.; Choi, E.; Kim, S.; Kim, D.S.; Kim, J.H.; Chang, S.; Choi, J.S.; Park, K.J.; Roh, K.-B.; Lee, J. Oxidative stress-protective and anti-melanogenic effects of loliolide and ethanol extract from fresh water green algae, *Prasiola japonica*. *Int. J. Mol. Sci.* **2018**, *19*, 2825. [[CrossRef](#)] [[PubMed](#)]
6. Choi, E.; Yi, Y.S.; Lee, J.; Park, S.H.; Kim, S.; Hossain, M.A.; Jang, S.; Choi, Y.I.; Park, K.J.; Kim, D.S.; et al. Anti-apoptotic and anti-inflammatory activities of edible fresh water algae *Prasiola japonica* in UVB-irradiated skin keratinocytes. *Am. J. Chin. Med.* **2019**, *47*, 1853–1868. [[CrossRef](#)]
7. Lee, C.Y.; Park, S.H.; Lim, H.Y.; Jang, S.G.; Park, K.J.; Kim, D.S.; Kim, J.H.; Cho, J.Y. In vivo anti-inflammatory effects of *Prasiola japonica* ethanol extract. *J. Funct. Foods* **2021**, *80*, 104440. [[CrossRef](#)]
8. Rahmawati, L.; Park, S.H.; Kim, D.S.; Lee, H.P.; Aziz, N.; Lee, C.Y.; Kim, S.A.; Jang, S.G.; Kim, D.S.; Cho, J.Y. Anti-inflammatory activities of the ethanol extract of *Prasiola japonica*, an edible freshwater green algae, and its various solvent fractions in lps-induced macrophages and carrageenan-induced paw edema via the ap-1 pathway. *Molecules* **2021**, *27*, 194. [[CrossRef](#)]
9. Baek, K.S.; Yi, Y.S.; Son, Y.J.; Yoo, S.; Sung, N.Y.; Kim, Y.; Hong, S.; Aravinthan, A.; Kim, J.H.; Cho, J.Y. In vitro and in vivo anti-inflammatory activities of Korean Red Ginseng-derived components. *J. Ginseng Res.* **2016**, *40*, 437–444. [[CrossRef](#)]
10. Xue, Q.; He, N.; Wang, Z.; Fu, X.; Aung, L.H.H.; Liu, Y.; Li, M.; Cho, J.Y.; Yang, Y.; Yu, T. Functional roles and mechanisms of ginsenosides from *Panax ginseng* in atherosclerosis. *J. Ginseng Res.* **2021**, *45*, 22–31. [[CrossRef](#)]
11. Kim, J.H.; Yi, Y.S.; Kim, M.Y.; Cho, J.Y. Role of ginsenosides, the main active components of *Panax ginseng*, in inflammatory responses and diseases. *J. Ginseng Res.* **2017**, *41*, 435–443. [[CrossRef](#)] [[PubMed](#)]
12. Han, C.; Hong, Y.C. Decrease in ambient fine particulate matter during COVID-19 crisis and corresponding health benefits in Seoul, Korea. *Int. J. Environ. Res. Public Health* **2020**, *17*, 5279. [[CrossRef](#)] [[PubMed](#)]
13. Fernando, I.P.S.; Jayawardena, T.U.; Kim, H.S.; Lee, W.W.; Vaas, A.; De Silva, H.I.C.; Abayaweera, G.S.; Nanayakkara, C.M.; Abeytunga, D.T.U.; Lee, D.S.; et al. Beijing urban particulate matter-induced injury and inflammation in human lung epithelial cells and the protective effects of fucosterol from *Sargassum binderi* (Sonder ex J. Agardh). *Environ. Res.* **2019**, *172*, 150–158. [[CrossRef](#)] [[PubMed](#)]
14. Ghio, A.J.; Smith, C.B.; Madden, M.C. Diesel exhaust particles and airway inflammation. *Curr. Opin. Pulm. Med.* **2012**, *18*, 144–150. [[CrossRef](#)] [[PubMed](#)]
15. Xu, M.; Zhao, X.; Zhao, S.; Yang, Z.; Yuan, W.; Han, H.; Zhang, B.; Zhou, L.; Zheng, S.; Li, M.D. Landscape analysis of Incrnas shows that ddx11-as1 promotes cell-cycle progression in liver cancer through the parp1/p53 axis. *Cancer Lett.* **2021**, *520*, 282–294. [[CrossRef](#)]
16. Hamanaka, R.B.; Mutlu, G.M. Particulate matter air pollution: Effects on the cardiovascular system. *Front. Endocrinol.* **2018**, *9*, 680. [[CrossRef](#)]
17. Tong, S. Air pollution and disease burden. *Lancet Planet. Health* **2019**, *3*, e49–e50. [[CrossRef](#)]
18. Orellano, P.; Reynoso, J.; Quaranta, N.; Bardach, A.; Ciapponi, A. Short-term exposure to particulate matter (PM10 and PM2.5), nitrogen dioxide (NO2), and ozone (O3) and all-cause and cause-specific mortality: Systematic review and meta-analysis. *Environ. Int.* **2020**, *142*, 105876. [[CrossRef](#)]
19. Ziou, M.; Tham, R.; Wheeler, A.J.; Zosky, G.R.; Stephens, N.; Johnston, F.H. Outdoor particulate matter exposure and upper respiratory tract infections in children and adolescents: A systematic review and meta-analysis. *Environ. Res.* **2022**, *210*, 112969. [[CrossRef](#)]
20. Xing, Y.F.; Xu, Y.H.; Shi, M.H.; Lian, Y.X. The impact of PM2.5 on the human respiratory system. *J. Thorac. Dis.* **2016**, *8*, E69–E74.
21. Migliaccio, C.T.; Kobos, E.; King, Q.O.; Porter, V.; Jessop, F.; Ward, T. Adverse effects of wood smoke PM2.5 exposure on macrophage functions. *Inhal. Toxicol.* **2013**, *25*, 67–76. [[CrossRef](#)]
22. Psoter, K.J.; De Roos, A.J.; Mayer, J.D.; Kaufman, J.D.; Wakefield, J.; Rosenfeld, M. Fine particulate matter exposure and initial *Pseudomonas aeruginosa* acquisition in cystic fibrosis. *Ann. Am. Thorac. Soc.* **2015**, *12*, 385–391. [[CrossRef](#)] [[PubMed](#)]

23. Mushtaq, N.; Ezzati, M.; Hall, L.; Dickson, I.; Kirwan, M.; Png, K.M.; Mudway, I.S.; Grigg, J. Adhesion of *Streptococcus pneumoniae* to human airway epithelial cells exposed to urban particulate matter. *J. Allergy Clin. Immunol.* **2011**, *127*, 1236–1242. [\[CrossRef\]](#) [\[PubMed\]](#)
24. Chen, X.; Liu, J.; Zhou, J.; Wang, J.; Chen, C.; Song, Y.; Pan, J. Urban particulate matter (PM) suppresses airway antibacterial defence. *Respir. Res.* **2018**, *19*, 5. [\[CrossRef\]](#) [\[PubMed\]](#)
25. Guarnieri, M.; Balmes, J.R. Outdoor air pollution and asthma. *Lancet* **2014**, *383*, 1581–1592. [\[CrossRef\]](#)
26. Brook, R.D.; Rajagopalan, S.; Pope, C.A., III; Brook, J.R.; Bhatnagar, A.; Diez-Roux, A.V.; Holguin, F.; Hong, Y.; Luepker, R.V.; Mittleman, M.A.; et al. Particulate matter air pollution and cardiovascular disease: An update to the scientific statement from the american heart association. *Circulation* **2010**, *121*, 2331–2378. [\[CrossRef\]](#)
27. Barrier, M.; Begorre, M.A.; Baudrimont, I.; Dubois, M.; Freund-Michel, V.; Marthan, R.; Savineau, J.P.; Muller, B.; Courtois, A. Involvement of heme oxygenase-1 in particulate matter-induced impairment of no-dependent relaxation in rat intralobar pulmonary arteries. *Toxicol. In Vitro* **2016**, *32*, 205–211. [\[CrossRef\]](#)
28. Beauchef, G.; Favre-Mercuret, M.; Blanc, B.; Fitoussi, R.; Vié, K.; Compagnone, N. Effect of red panax ginseng on mitochondrial dynamics and bioenergetics in hacat cells exposed to urban pollutants. *J. Cosmet. Dermatol. Sci. Appl.* **2021**, *11*, 84–95.
29. Nowak, B.; Majka, G.; Srottek, M.; Skalkowska, A.; Marcinkiewicz, J. The effect of inhaled air particulate matter srm 1648a on the development of mild collagen-induced arthritis in dba/j mice. *Arch. Immunol. Ther. Exp.* **2022**, *70*, 17. [\[CrossRef\]](#)
30. Gawda, A.; Majka, G.; Nowak, B.; Srottek, M.; Walczewska, M.; Marcinkiewicz, J. Air particulate matter srm 1648a primes macrophages to hyperinflammatory response after lps stimulation. *Inflamm. Res.* **2018**, *67*, 765–776. [\[CrossRef\]](#)
31. Lorz, L.R.; Kim, D.; Kim, M.Y.; Cho, J.Y. Panax ginseng-derived fraction biogf1k reduces atopic dermatitis responses via suppression of mitogen-activated protein kinase signaling pathway. *J. Ginseng Res.* **2020**, *44*, 453–460. [\[CrossRef\]](#) [\[PubMed\]](#)
32. Song, C.; Lorz, L.R.; Lee, J.; Cho, J.Y. In vitro photoprotective, anti-inflammatory, moisturizing, and antimelanogenic effects of a methanolic extract of chrysophyllum lucentifolium cronquist. *Plants* **2021**, *11*, 94. [\[CrossRef\]](#) [\[PubMed\]](#)
33. Lee, H.P.; Kim, D.S.; Park, S.H.; Shin, C.Y.; Woo, J.J.; Kim, J.W.; An, R.B.; Lee, C.; Cho, J.Y. Antioxidant Capacity of *Potentilla paradoxa* Nutt. and Its Beneficial Effects Related to Anti-Aging in HaCaT and B16F10 Cells. *Plants* **2022**, *11*, 873. [\[CrossRef\]](#) [\[PubMed\]](#)
34. Lee, J.O.; Hwang, S.H.; Shen, T.; Kim, J.H.; You, L.; Hu, W.; Cho, J.Y. Enhancement of skin barrier and hydration-related molecules by protopanaxatriol in human keratinocytes. *J. Ginseng Res.* **2021**, *45*, 354–360. [\[CrossRef\]](#)
35. Jang, W.Y.; Lee, H.P.; Kim, S.A.; Huang, L.; Yoon, J.H.; Shin, C.Y.; Mitra, A.; Kim, H.G.; Cho, J.Y. *Angiopteris cochinchinensis* de vriese ameliorates lps-induced acute lung injury via src inhibition. *Plants* **2022**, *11*, 1306. [\[CrossRef\]](#)
36. Mitra, A.; Rahmawati, L.; Lee, H.P.; Kim, S.A.; Han, C.K.; Hyun, S.H.; Cho, J.Y. Korean red ginseng water extract inhibits cadmium-induced lung injury via suppressing mapk/erk1/2/ap-1 pathway. *J. Ginseng Res.* **2022**, *46*, 690–699. [\[CrossRef\]](#)
37. Matute-Bello, G.; Downey, G.; Moore, B.B.; Groshong, S.D.; Matthay, M.A.; Slutsky, A.S.; Kuebler, W.M.; Acute Lung Injury in Animals Study Group. An official american thoracic society workshop report: Features and measurements of experimental acute lung injury in animals. *Am. J. Respir. Cell Mol. Biol.* **2011**, *44*, 725–738. [\[CrossRef\]](#)
38. Kim, J.K.; Choi, E.; Hong, Y.H.; Kim, H.; Jang, Y.J.; Lee, J.S.; Choung, E.S.; Woo, B.Y.; Hong, Y.D.; Lee, S.; et al. Syk/nf-kappab-targeted anti-inflammatory activity of *Melicope accedens* (Blume) T.G. Hartley methanol extract. *J. Ethnopharmacol.* **2021**, *271*, 113887. [\[CrossRef\]](#)
39. Choi, W.; Kim, H.S.; Park, S.H.; Kim, D.; Hong, Y.D.; Kim, J.H.; Cho, J.Y. Syringaresinol derived from Panax ginseng berry attenuates oxidative stress-induced skin aging via autophagy. *J. Ginseng Res.* **2022**, *46*, 536–542. [\[CrossRef\]](#)
40. Park, S.K.; Yeon, S.H.; Choi, M.R.; Choi, S.H.; Lee, S.B.; Rha, K.S.; Kim, Y.M. Urban particulate matters may affect endoplasmic reticulum stress and tight junction disruption in nasal epithelial cells. *Am. J. Rhinol. Allergy* **2021**, *35*, 817–829. [\[CrossRef\]](#)
41. Van Vyve, T.; Chanez, P.; Bernard, A.; Bousquet, J.; Godard, P.; Lauwerijs, R.; Sibille, Y. Protein content in bronchoalveolar lavage fluid of patients with asthma and control subjects. *J. Allergy Clin. Immunol.* **1995**, *95*, 60–68. [\[CrossRef\]](#) [\[PubMed\]](#)
42. Liu, T.; Zhang, L.; Joo, D.; Sun, S.-C. Nf-kb signaling in inflammation. *Signal Transduct. Target. Ther.* **2017**, *2*, 17023. [\[CrossRef\]](#) [\[PubMed\]](#)
43. Mulero, M.C.; Huxford, T.; Ghosh, G.J.S.I. Nf-kb, ikb, and ikk: Integral components of immune system signaling. *Adv. Exp. Med. Biol.* **2019**, *1172*, 207–226. [\[PubMed\]](#)
44. Morgan, M.J.; Liu, Z.G. Crosstalk of reactive oxygen species and nf-kappab signaling. *Cell Res.* **2011**, *21*, 103–115. [\[CrossRef\]](#) [\[PubMed\]](#)
45. Sun, S.; Frontini, F.; Qi, W.; Hariharan, A.; Ronner, M.; Wipplinger, M.; Blanquart, C.; Rehrauer, H.; Fonteneau, J.F.; Felley-Bosco, E. Endogenous retrovirus expression activates type-i interferon signaling in an experimental mouse model of mesothelioma development. *Cancer Lett.* **2021**, *507*, 26–38. [\[CrossRef\]](#) [\[PubMed\]](#)
46. Casal-Mourino, A.; Ruano-Ravina, A.; Torres-Duran, M.; Parente-Lamelas, I.; Provencio-Pulla, M.; Castro-Anon, O.; Vidal-Garcia, I.; Pena-Alvarez, C.; Abal-Arca, J.; Pineiro-Lamas, M.; et al. Lung cancer survival in never-smokers and exposure to residential radon: Results of the lcrins study. *Cancer Lett.* **2020**, *487*, 21–26. [\[CrossRef\]](#) [\[PubMed\]](#)
47. Anderson, J.O.; Thundiyil, J.G.; Stolbach, A. Clearing the air: A review of the effects of particulate matter air pollution on human health. *J. Med. Toxicol.* **2012**, *8*, 166–175. [\[CrossRef\]](#) [\[PubMed\]](#)

48. Marshall, J. Pm 2.5. *Proc. Natl. Acad. Sci. USA* **2013**, *110*, 8756. [[CrossRef](#)]
49. Xu, X.C.; Wu, Y.F.; Zhou, J.S.; Chen, H.P.; Wang, Y.; Li, Z.Y.; Zhao, Y.; Shen, H.H.; Chen, Z.H. Autophagy inhibitors suppress environmental particulate matter-induced airway inflammation. *Toxicol. Lett.* **2017**, *280*, 206–212. [[CrossRef](#)]
50. Xia, Y.; Dolgor, S.; Jiang, S.; Fan, R.; Wang, Y.; Wang, Y.; Tang, J.; Zhang, Y.; He, R.L.; Yu, B.; et al. Yiqifumai lyophilized injection attenuates particulate matter-induced acute lung injury in mice via tlr4-mtor-autophagy pathway. *Biomed. Pharmacother.* **2018**, *108*, 906–913. [[CrossRef](#)]
51. Wang, Y.; Tang, M. Integrative analysis of mrnas, mirnas and lncrnas in urban particulate matter srm 1648a-treated ea.Hy926 human endothelial cells. *Chemosphere* **2019**, *233*, 711–723. [[CrossRef](#)] [[PubMed](#)]
52. Chen, H.; Zhou, X.H.; Li, J.R.; Zheng, T.H.; Yao, F.B.; Gao, B.; Xue, T.C. Neutrophils: Driving inflammation during the development of hepatocellular carcinoma. *Cancer Lett.* **2021**, *522*, 22–31. [[CrossRef](#)] [[PubMed](#)]
53. Chen, Y.; Ho, L.; Tergaonkar, V. Sorf-encoded micropeptides: New players in inflammation, metabolism, and precision medicine. *Cancer Lett.* **2021**, *500*, 263–270. [[CrossRef](#)] [[PubMed](#)]
54. Chan, Y.L.; Wang, B.; Chen, H.; Ho, K.F.; Cao, J.; Hai, G.; Jalaludin, B.; Herbert, C.; Thomas, P.S.; Saad, S.; et al. Pulmonary inflammation induced by low-dose particulate matter exposure in mice. *Am. J. Physiol. Lung Cell. Mol. Physiol.* **2019**, *317*, L424–L430. [[CrossRef](#)] [[PubMed](#)]
55. Wu, Y.X.; He, H.Q.; Nie, Y.J.; Ding, Y.H.; Sun, L.; Qian, F. Protostemonine effectively attenuates lipopolysaccharide-induced acute lung injury in mice. *Acta Pharmacol. Sin.* **2018**, *39*, 85–96. [[CrossRef](#)] [[PubMed](#)]
56. Sun, H.; Li, Q.; Jin, Y.; Qiao, H.J.E.; Pathology, M. Associations of tumor necrosis factor- α polymorphisms with the risk of asthma: A meta-analysis. *Exp. Mol. Pathol.* **2018**, *105*, 411–416. [[CrossRef](#)]
57. Lai, W.-Y.; Wang, J.-W.; Huang, B.-T.; Lin, E.P.-Y.; Yang, P.-C.J.T. A novel tnf- α -targeting aptamer for tnf- α -mediated acute lung injury and acute liver failure. *Theranostics* **2019**, *9*, 1741. [[CrossRef](#)]
58. Leija-Martínez, J.J.; Huang, F.; Del-Río-Navarro, B.E.; Sánchez-Muñoz, F.; Muñoz-Hernández, O.; Giacomani-Martínez, A.; Hall-Mondragon, M.S.; Espinosa-Velazquez, D.J.M.h. Il-17a and tnf- α as potential biomarkers for acute respiratory distress syndrome and mortality in patients with obesity and COVID-19. *Med. Hypotheses* **2020**, *144*, 109935. [[CrossRef](#)]
59. Lee, S.G.; An, J.H.; Kim, D.H.; Yoon, M.S.; Lee, H.J. A case of interstitial lung disease and autoimmune thyroiditis associated with ustekinumab. *Acta Derm. Venereol.* **2019**, *99*, 331–332. [[CrossRef](#)]
60. Mirzaei, S.; Zarrabi, A.; Hashemi, F.; Zabolian, A.; Saleki, H.; Ranjbar, A.; Seyed Saleh, S.H.; Bagherian, M.; Sharifzadeh, S.O.; Hushmandi, K.; et al. Regulation of nuclear factor-kappa b (nf-kb) signaling pathway by non-coding RNAs in cancer: Inhibiting or promoting carcinogenesis? *Cancer Lett.* **2021**, *509*, 63–80. [[CrossRef](#)]
61. Luo, J.; Ma, Q.; Tang, H.; Zou, X.; Guo, X.; Hu, Y.; Zhou, K.; Liu, R. Ltb4 promotes acute lung injury via upregulating the plcepsilon-1/tlr4/nf-kappa b pathway in one-lung ventilation. *Dis. Markers* **2022**, *2022*, 1839341. [[CrossRef](#)] [[PubMed](#)]
62. Zeng, Y.; Zhu, G.; Zhu, M.; Song, J.; Cai, H.; Song, Y.; Wang, J.; Jin, M. Edaravone Attenuated Particulate Matter-Induced Lung Inflammation by Inhibiting ROS-NF- κ B Signaling Pathway. *Oxid. Med. Cell Longev.* **2022**, *2022*, 6908884. [[CrossRef](#)] [[PubMed](#)]
63. Su, V.Y.-F.; Lin, C.-S.; Hung, S.-C.; Yang, K.-Y. Mesenchymal stem cell-conditioned medium induces neutrophil apoptosis associated with inhibition of the nf-kb pathway in endotoxin-induced acute lung injury. *Int. J. Mol. Sci.* **2019**, *20*, 2208. [[CrossRef](#)] [[PubMed](#)]
64. Kwon, K.; Park, S.H.; Han, B.S.; Oh, S.W.; Lee, S.E.; Yoo, J.A.; Park, S.J.; Kim, J.; Kim, J.W.; Cho, J.Y.; et al. Negative cellular effects of urban particulate matter on human keratinocytes are mediated by p38 mapk and nf-kappa b-dependent expression of trpv 1. *Int. J. Mol. Sci.* **2018**, *19*, 2660. [[CrossRef](#)] [[PubMed](#)]
65. Nagumo, Y.; Kandori, S.; Tanuma, K.; Nitta, S.; Chihara, I.; Shiga, M.; Hoshi, A.; Negoro, H.; Kojima, T.; Mathis, B.J.; et al. Pld1 promotes tumor invasion by regulation of mmp-13 expression via nf-kappa b signaling in bladder cancer. *Cancer Lett.* **2021**, *511*, 15–25. [[CrossRef](#)]
66. Sanjeeva, K.; Kim, H.-S.; Lee, H.-G.; Jayawardena, T.U.; Nagahawatta, D.; Yang, H.-W.; Udayanga, D.; Kim, J.-I.; Jeon, Y.-J. 3-hydroxy-5, 6-epoxy- β -ionone isolated from invasive harmful brown seaweed *Sargassum horneri* protects mh-s mouse lung cells from urban particulate matter-induced inflammation. *Appl. Sci.* **2021**, *11*, 10929. [[CrossRef](#)]
67. He, M.; Ichinose, T.; Kobayashi, M.; Arashidani, K.; Yoshida, S.; Nishikawa, M.; Takano, H.; Sun, G.; Shibamoto, T. Differences in allergic inflammatory responses between urban pm2. 5 and fine particle derived from desert-dust in murine lungs. *Toxicol Appl. Pharmacol.* **2016**, *297*, 41–55. [[CrossRef](#)]
68. Wang, Y.W.; Wu, Y.H.; Zhang, J.Z.; Tang, J.H.; Fan, R.P.; Li, F.; Yu, B.Y.; Kou, J.P.; Zhang, Y.Y. Ruscogenin attenuates particulate matter-induced acute lung injury in mice via protecting pulmonary endothelial barrier and inhibiting tlr4 signaling pathway. *Acta Pharmacol. Sin.* **2021**, *42*, 726–734. [[CrossRef](#)]
69. Ma, D.; Zhan, D.; Fu, Y.; Wei, S.; Lal, B.; Wang, J.; Li, Y.; Lopez-Bertoni, H.; Yalcin, F.; Dzaye, O.; et al. Mutant idh1 promotes phagocytic function of microglia/macrophages in gliomas by downregulating icam1. *Cancer Lett.* **2021**, *517*, 35–45. [[CrossRef](#)]
70. Lu, H.; Fu, C.; Kong, S.; Wang, X.; Sun, L.; Lin, Z.; Luo, P.; Jin, H. Maltol prevents the progression of osteoarthritis by targeting pi3k/akt/nf-kappa b pathway: In vitro and in vivo studies. *J. Cell. Mol. Med.* **2021**, *25*, 499–509. [[CrossRef](#)]

71. Kim, B.-H.; Cho, I.-A.; Kang, K.-R.; Lee, S.-Y.; Jung, S.-Y.; Kim, J.-S.; Kim, S.-G. Bavachin counteracts receptor activator of nuclear factor- κ b-induced osteoclastogenesis through the suppression of nuclear factor- κ b signaling pathway in raw264.7 cells. *Oral Biol. Res.* **2018**, *42*, 130–139. [[CrossRef](#)]
72. Lin, Z.; Wu, D.; Huang, L.; Jiang, C.; Pan, T.; Kang, X.; Pan, J. Nobiletin inhibits il-1 β -induced inflammation in chondrocytes via suppression of nf- κ b signaling and attenuates osteoarthritis in mice. *Front. Pharmacol.* **2019**, *10*, 570. [[CrossRef](#)] [[PubMed](#)]

Disclaimer/Publisher’s Note: The statements, opinions and data contained in all publications are solely those of the individual author(s) and contributor(s) and not of MDPI and/or the editor(s). MDPI and/or the editor(s) disclaim responsibility for any injury to people or property resulting from any ideas, methods, instructions or products referred to in the content.